Supramolecular Chemistry

DOI: 10.1002/ange.201405652

Water Encapsulation by Nanomicelles**

Iker León, Judith Millán, Emilio J. Cocinero, Alberto Lesarri, and José A. Fernández**

Abstract: *Reported is the hydration of nanomicelles in the gas-phase using spectroscopic methods and quantum chemical calculations. A fine-tuning of the experimental conditions allowed formation of a propofol trimer and tetramer with a water molecule and to determine the structure of the aggregates. Their electronic and IR spectra were obtained using mass-resolved laser spectroscopy, together with the number of conformational isomers for each stoichiometry. Interpretation of the spectra in the light of high-level calculations allowed determination of the cluster's structure and demonstration that the trimer of propofol with a water molecule forms cyclic hydrogen-bond networks but, on the other hand, the tetramer is big enough to encapsulate the water molecule inside its hydrophilic core. Furthermore, these hydrated nanomicelles present an unusually high binding energy, thus reflecting their high stability and their capability to trap water inside.*

Reverse micelles (RMs) are thermodynamically stable, nanometer-sized assemblies of amphiphilic molecules which are organized with their polar part within the inner core and their apolar part on the outside.[1,2] RMs are thus able to encapsulate microscopic pools of water while the apolar part remains in contact with an organic solvent.[3,4] This function allows proteins and other hydrophilic molecules to be solubilized in an aqueous microenvironment while organic reactants and products remain in the bulk organic phase. Because of their important biological role, several applications have been found for RMs: they can be used as reaction systems for enzymatic catalysis,[5,6] drug delivery,[7,8] solvent-based extraction of proteins,[9,10] industrial processes,[11] microenvironment for discovery of protein structures,[12] protein refolding,[13,14] or even treated as models of membrane systems for the separation of proteins,[15] etc. In the past three decades, the application of RMs for bioseparation has attracted considerable attention because of the technique's potential usefulness in downstream processing for the large-scale separation of biomolecules.[16]

The presence of water of hydration in RMs is of particular importance as it plays key roles in stabilizing the structure of proteins.[17] The microenvironment in which the protein is solubilized within the micelles has distinct physicochemical properties compared to those of the bulk aqueous solution, and hence understanding their interactions at a molecular level is critical to modelling the encapsulation process. In a previous work, we studied the formation of micelles in the gas phase by using an uncommon reductionist approach.[18] We used up to six molecules of propofol to form micellar aggregates and observed the critical balance between hydrogen-bond interactions and noncovalent forces in the control of the aggregation process. The work clearly reflected the importance of multiple weak noncovalent interactions to the final shape of the biological supramolecular structures. In fact, the correlation between a larger red-shift of the bonded OH moieties in the IR laser experiments and the number of propofol molecules reflected the strong cooperative effects present in these micelles. In a quest for understanding what the driving forces are for the encapsulation of water within these supramolecular structures, we adopted the same approach, that is, introducing water molecules into other nanomicelles in a controlled and sequential way. Herein, we present our results for the propofol trimer and tetramer with the addition of a water molecule; these units are among the biggest possible systems allowing vibrational resolution.[18–20]

The structure of the cluster was investigated using mass-resolved laser excitation spectroscopy. Figure 1 shows the two-color REMPI (resonance enhanced multiphoton ionization) spectrum of P_3W_1 and P_4W_1 (where P = propofol and W = water), obtained integrating the corresponding mass-channel while the pump laser is scanned along the 35900–36400 cm^{-1} UV region. The REMPI spectrum provides a signature of the electronic $S_1 \leftarrow S_0$ transition of the neutral molecule with vibrational resolution. For P_3W_1 there are numerous vibronic bands. The use of UV/UV double-resonance (hole burning) determines the number of conformational isomers contributing to this mass-channel. Clearly, the numerous vibronic bands in the spectrum are due to the contribution of two isomers (Figure 1a; red and blue traces obtained probing the transitions at 36003 and 36205 cm^{-1}). Unfortunately, the low signal for P_4W_1 precluded obtaining a clear hole-burning spectrum. For this reason, all the vibrational transitions in the REMPI spectrum

[*] Dr. I. León, Dr. E. J. Cocinero, Dr. J. A. Fernández
Dep. Química Física, Fac. Ciencia y Tecnología
Universidad del País Vasco (UPV/EHU)
B. Sarriena, s/n, 48940 Leioa (Spain)
E-mail: iker.leon@ehu.es
josea.fernandez@ehu.es
Homepage: https://sites.google.com/site/gesemupv/
Dr. J. Millán
Dep. Química, Facultad de Ciencias, Estudios Agroalimentarios e Informática, Universidad de La Rioja, 26006 Logroño (Spain)
Prof. A. Lesarri
Dep. de Química Física y Química Inorgánica, Universidad de Valladolid, 47011 Valladolid (Spain)

[**] We thank the Spanish MICINN and MINECO (CTQ2012-39132 and CTQ2011-22923), the Basque Government (IT520-10), and UPV/EHU (UFI 11/23) for funding. E.J.C. also thanks the MICINN for a "Ramón y Cajal" contract and I.L. thanks the GV for pre- and post-doctoral fellowships. Computational resources and laser facilities from the SGI/IZO-SGIker and i2BASQUE were used for this work. Technical support provided by the Laser Facility of the SGIKER (UPV/EHU, MICINN, GV/EJ, ESF) is also gratefully acknowledged.

Supporting information for this article is available on the WWW under http://dx.doi.org/10.1002/anie.201405652.

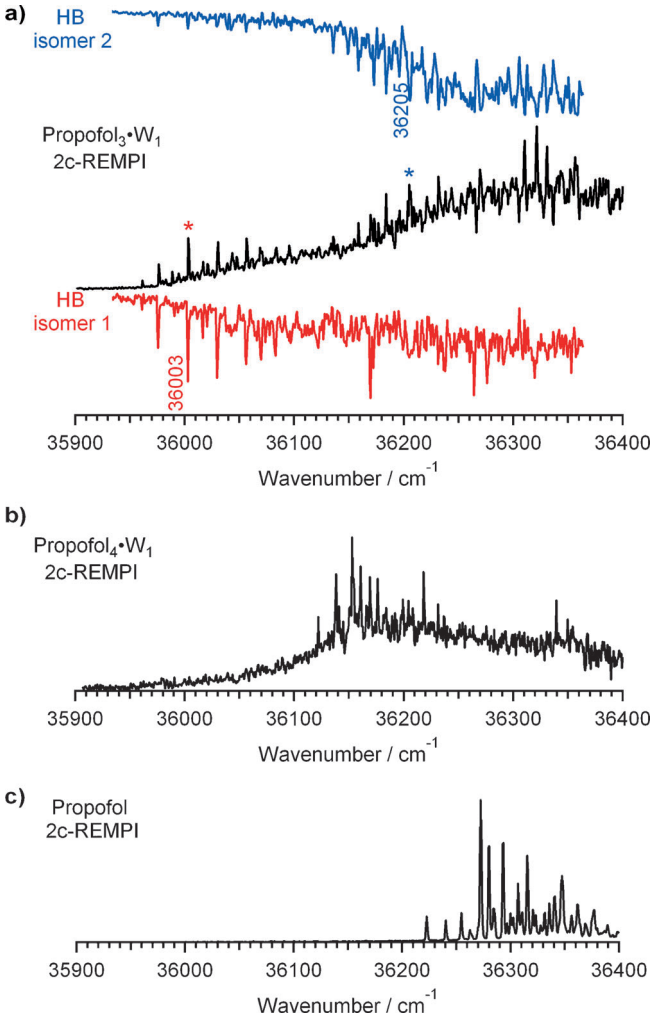

Figure 1. a) Comparison between the two-color REMPI spectrum of P_3W_1 and the hole-burning traces obtained probing the transitions marked with asterisks. The existence of two isomers is demonstrated. Two-color REMPI spectrum of b) P_4W_1 and c) propofol. The REMPI spectra appear as positive peaks while the hole-burning traces appear as negative (depleted) peaks.

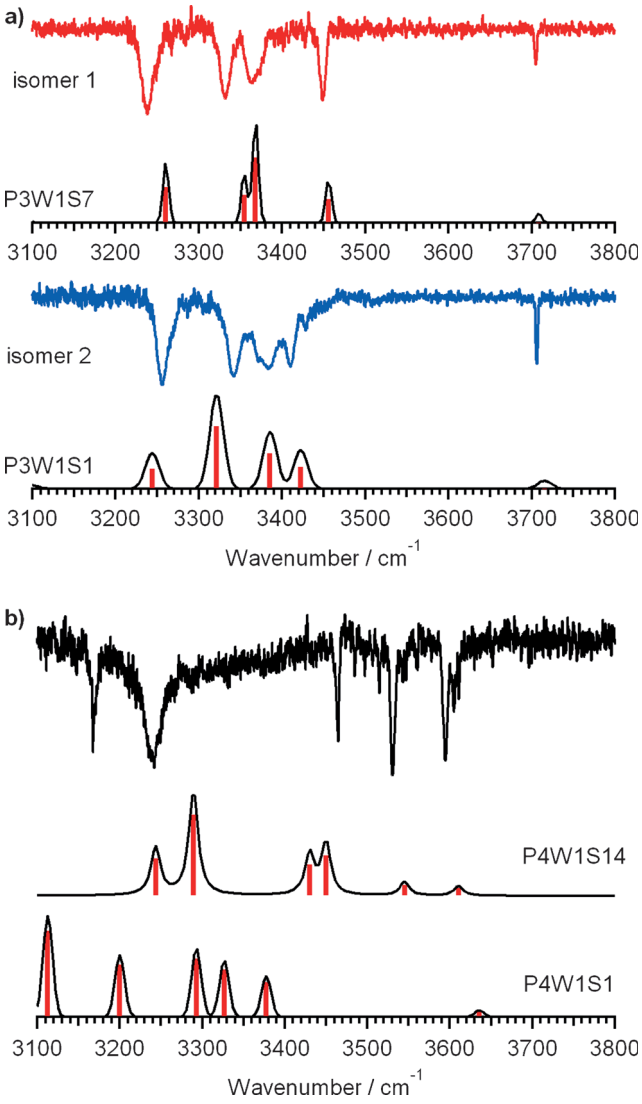

Figure 2. a) IR/UV spectra of the two detected isomers of P_3W_1. The spectra simulated for the assigned structures are shown for comparison. b) IR/UV spectra of P_4W_1. The spectra for the assigned structure and the global minimum are shown for comparison. The calculation was done at M06-2X/6-31+G(d) level. A correction factor of 0.955 was employed.

of Figure 1b were probed systematically, but no IR spectrum different from that discussed below was obtained, which is consistent with the presence of a single conformer.

Vibrational spectroscopy is extensively used to study the molecular structure and intermolecular interactions of molecular clusters. One of the most powerful spectroscopic probes of hydrogen-bonding networks is the OH/NH stretch region of the infrared, as the vibrational frequencies of the fundamental OH/NH stretch are sensitive functions of the number, type, and strength of hydrogen bonds in which each OH/NH group participates. In particular, IR-UV double-resonance laser experiments constitute a highly sensitive and selective method to record the vibrational spectra of molecular clusters with both mass and conformational specificity.[21] Figure 2 shows the IR spectrum obtained for each of the two isomers of P_3W_1 and for the singly detected isomer in P_4W_1. To our knowledge, this is the largest system for which the mass-resolved conformer-specific IR spectrum has been obtained and assigned.

The two IR spectra of P_3W_1 shown in Figure 2a are very similar, thus indicating that the two isomers have a similar structure. Isomer 1 presents a single peak at 3705 cm^{-1} which is a result of the free OH stretching mode of the water molecule and there are four peaks resolved to the baseline and red-shifted to 3238, 3331, 3365 and 3449 cm^{-1}, thus indicating that these OH groups are involved in a moderately strong hydrogen bond. Likewise, the second isomer presents an OH stretching mode at 3706 cm^{-1} which represents the free water OH, and four peaks at 3256, 3342, 3382 and 3410 cm^{-1} in the red-most part of the spectrum. The absence of any peak between the hydrogen-bonded bands and the free OH stretching mode is known as the "window region"[22] and it is a fingerprint for clusters where the OH groups are forming a cyclic arrangement.

To aid in the identification of the two detected isomers, the conformational landscape of P_3W_1 was explored by molecular mechanics (MM) and density-fuctional theory (DFT) using a procedure described elsewhere.[23,24] Thousands of structures were first found within a 20 kJ mol^{-1} stability window using MM. Most of the structures are very similar, differing slightly in the position of the propofol molecules or in the orientation of the free OH group of water. The structures were grouped into families and representative members of each family, as well as the most stable structures were subject to full optimization using DFT (M06-2X/6-31 + G(d) calculation level). The M06-2X functional has proven to be computationally effective for the molecular sizes proposed here, satisfactorily accounting for the effects of nonbonding interactions.[25–27] Figure S1 of the Supporting Information shows the resulting 36 structures which are labelled P3W1Sn, $n = 1,2\ldots$, starting with the most stable one. Comparison between the spectra predicted for the calculated structures and the experimental traces allows to propose an assignment for the detected species. Figure 2a shows that only structures whose OH groups are forming a cyclic arrangement are able to reproduce the experimental observations for the P_3W_1 conformers. Even though both conformers are very similar, small variations in the position of the molecules within the cluster create a different environment for each OH group. These subtle differences can be photographed experimentally and the IR spectra of the two conformers can be compared, showing a qualitatively good match with the simulated predictions.

In contrast, the singly detected conformer of P_4W_1 shows a very interesting IR signature displaying several vibrational transitions scattered along the scanned region. These results are exciting, as they indicate that the cluster is no longer forming a cyclic hydrogen-bond network. Figure S3 of the Supporting Information shows the 49 calculated structures labelled as P4W1Sn, $n = 1,2\ldots$, starting with the most stable one. Additionally, Figure 2b shows the proposed assignment, together with another representative structure whose predicted spectrum does not reproduce the experimental observations. None of the calculated structures where the OH groups are forming a cyclic arrangement, present a spectrum that resembles the experimental trace recorded for this cluster. An example of this is the structure P4W1S1, which is also predicted as the global minimum. In contrast, acyclic structures such as P4W1S14 fairly reproduce the spectrum of P_4W_1, even taking into account that the conformational landscape is extremely large, and thus it is not possible to analyze all possible configurations. In any case, the absence of the window region is irrefutable proof of the noncyclic nature of the hydrogen-bond network. Furthermore, there is no free OH stretching mode for the water molecule, meaning that it is acting as a double donor. The absence of the most stable structure could be due to entropic or kinetic reasons as a result of collisions of the P3W1 cluster with another propofol molecule during the formation process.

The assigned structures are collected in Figure 3. The only difference between the two isomers of P_3W_1 lies in the relative position of the propofol molecules. In a previous paper on gas-phase nanosized micelles our results highlighted that their

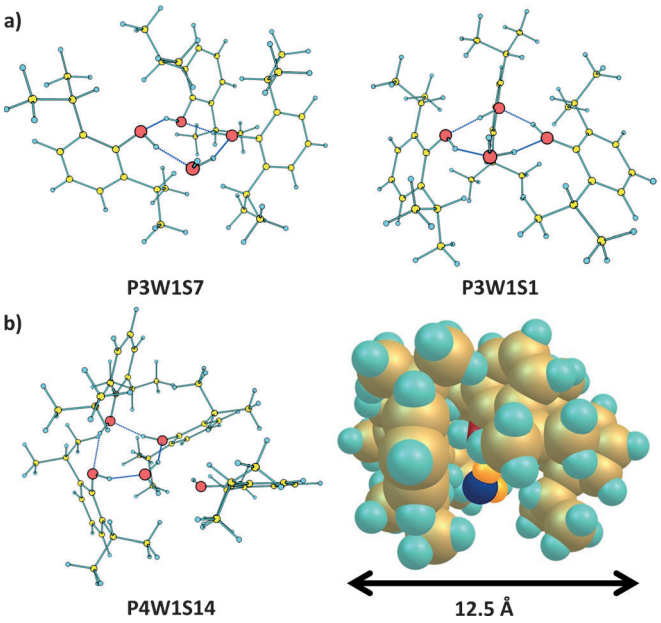

Figure 3. Comparison between the detected a) P_3W_1 and b) P_4W_1 isomers. The globular structure of P_4W_1 is also shown, together with the diameter of the cluster (H light blue, C brown, O red). In the sphere's molecular model water atoms are depicted in different colors for easy visualization (O dark blue, H orange).

shape was not only a result of the hydrogen bonds, but that the dispersive forces also played a fundamental role.[18] In fact, the final shape of these micellar nanostructures was mainly due to the less directive but more full-scale dispersive-force interactions. P_3W_1 falls into the same category and, while the hydrogen bonds play a substantial role in the construction of the micelles, it is the dispersive forces between the aromatic rings and CH—π interactions which gives the overall shape of these nanostructures. Additionally, the high binding energy of 141 kJ mol^{-1} in these structures is remarkable. Hence a lot of energy is required to break this arrangement, thus highlighting the capability of these micelles to solvate water molecules within the inner core.

To further test this hypothesis and in pursuit for understanding what the minimum size of a reverse micelle to encapsulate a water molecule is, the solvation of water into the tetramer micellar structure was done. Figure 3b shows that P_4W_1 is an important finding as, not only the water molecule unexpectedly enters the encapsulated part of the micelle, but that it is also able to displace the propofol tetramer (which has a binding energy of c.a 150 kJ mol^{-1}) to penetrate this nanomeric assembly. In fact, water is accommodated inside the micelle while the cluster still presents a lipophobic globular structure as shown in the spheres-model representation in Figure 3b. The results presented here are relevant as we provide the first evidence, at a molecular level, of how the RMs are able to encapsulate microscopic pools of water while the apolar unit remains outside the micelle. Furthermore, this particular arrangement still preserves an unusual high binding energy of 200 kJ mol^{-1}, thus highlighting that these peculiar nanosolvated micelles are extremely stable. Interestingly, while the interior of the molecule

accommodates the hydrophilic part of the OH moieties, the outside of the micelle remains practically unchanged, with a lipophobic region of 12.5 Å compared to the virtually identical size of the tetramer and very close to that of the pentamer (14.2 Å). The global cooperative effect of the weak, but multiple, interactions is reflected in the large spectral red-shift of some of the hydrogen-bonded OH groups, as well as in the unusually high binding energy, which is considerably much higher than that of the sum of the dimerization energy of each pair.

The extension of high-resolution studies to larger well-defined isolated nanomicelles will improve the description of molecular aggregation from a fundamental point of view, thus revealing how weak interactions collaborate to form large-scale structures. Our group is extending now these studies to different polyhydrated systems.

Received: May 26, 2014
Published online: July 17, 2014

Keywords: computational chemistry · IR spectroscopy · micelles · non-covalent interactions · supramolecular chemistry

[1] T. P. Hoar, J. H. Schulman, *Nature* **1943**, *152*, 102 – 104.
[2] M. B. Mathews, E. Hirschhorn, *J. Colloid Interface Sci.* **1953**, *8*, 86 – 93.
[3] R. Bru, A. Sánchez-Ferrer, F. García-Carmona, *Biochem. J.* **1995**, *310*, 721 – 739.
[4] P. Ball, *Nature* **1991**, *349*, 101 – 102.
[5] D. H. Zhang, Z. Guo, X. Y. Dong, Y. Sun, *Biotechnol. Prog.* **2007**, *23*, 108 – 115.
[6] J. F. Rathman, *Curr. Opin. Colloid Interface Sci.* **1996**, *1*, 514 – 518.
[7] V. P. Torchilin, *Pharm. Res.* **2007**, *24*, 1 – 16.
[8] F. Denat, Y. Diaz-Fernandez, L. Pasotti, N. Sok, P. Pallavicini, *Chem. Eur. J.* **2010**, *16*, 1289 – 1295.
[9] Y. Liu, X. Y. Dong, Y. Sun, *Sep. Purif. Technol.* **2007**, *53*, 289 – 295.
[10] P. L. Luisi, F. J. Bonner, A. Pellegrini, P. Wiget, R. Wolf, *Helv. Chim. Acta* **1979**, *62*, 740 – 748.
[11] B. L. Cushing, V. L. Kolesnichenko, C. J. O'Connor, *Chem. Rev.* **2004**, *104*, 3893 – 3946.
[12] K. Naoe, K. Noda, M. Kawagoe, M. Imai, *Colloids Surf. B* **2004**, *38*, 179 – 185.
[13] T. Ono, M. Nagatomo, T. Nagao, H. Ijima, K. Kawakami, *Biotechnol. Bioeng.* **2005**, *89*, 290 – 295.
[14] X. Y. Wu, Y. Liu, X. Y. Dong, Y. Sun, *Biotechnol. Prog.* **2006**, *22*, 499 – 504.
[15] Y. Nishii, T. Kinugasa, S. Nii, K. Takahashi, *J. Membr. Sci.* **2002**, *195*, 11 – 21.
[16] Y. Liu, X. Dong, Y. Sun, *Chin. J. Chem. Eng.* **2008**, *16*, 949 – 955.
[17] J. L. Finney, B. J. Gelati, I. C. Golton, J. M. Goodfellow, *Biophys. J.* **1980**, *32*, 17 – 30.
[18] I. León, J. Millán, E. J. Cocinero, A. Lesarri, J. A. Fernández, *Angew. Chem.* **2013**, *125*, 7926 – 7929; *Angew. Chem. Int. Ed.* **2013**, *52*, 7772 – 7775.
[19] P. Hobza, K. Muller-Dethlefs, *Non-Covalent Interactions*, RCS, London, **2010**.
[20] M. Saeki, S. Ishiuchi, M. Sakai, K. Hashimoto, M. Fujii, *J. Phys. Chem. A* **2010**, *114*, 11210 – 11215.
[21] R. H. Page, Y. R. Shen, Y. T. Lee, *J. Chem. Phys.* **1988**, *88*, 4621 – 4636.
[22] T. Ebata, *Bull. Chem. Soc. Jpn.* **2009**, *82*, 127 – 151.
[23] I. León, E. J. Cocinero, J. Millán, S. Jaeqx, A. Rijs, A. Lesarri, F. Castaño, J. A. Fernández, *Phys. Chem. Chem. Phys.* **2012**, *14*, 4398 – 4409.
[24] I. León, J. Millán, E. J. Cocinero, A. Lesarri, F. Castaño, J. A. Fernández, *Phys. Chem. Chem. Phys.* **2012**, *14*, 8956 – 8963.
[25] I. León, J. Millán, F. Castaño, J. A. Fernández, *ChemPhysChem* **2012**, *13*, 3819 – 3826.
[26] I. León, E. J. Cocinero, A. Lesarri, F. Castaño, J. A. Fernández, *J. Phys. Chem. A* **2012**, *116*, 8934 – 8941.
[27] I. León, E. J. Cocinero, A. M. Rijs, J. Millán, E. Alonso, A. Lesarri, J. A. Fernández, *Phys. Chem. Chem. Phys.* **2013**, *15*, 568 – 575.

